BALKAN JOURNAL OF ELECTRICAL & COMPUTER ENGINEERING, Vol. 8, No. 2, April 2020

Determination of Leakage Inductance Percentage for Gapped Iron-Core Shunt-Reactors with M4 Steel as Core Material

A. DÖNÜK

***Abstract*—Leakage inductance component has a significant importance in total inductance value of GISR. Neglecting this component in the design phase, results in an expensive and bulky core structure. Variation of leakage inductance component in percentage is determined and presented as graphical curves for M4 steel by applying energy method. FEA are performed for various GISR with several operating voltages and temperature rise values to determine the leakage inductance component. A design tool with Matlab/Guide is also developed for analytical calculations to obtain the physical dimensions for FEA. Graphical curves introduced to the literature in this work provide manufacturers or design engineers to perform fast, reliable and economical GISR design with an alternative material and offer variety.**

Index Terms— **Air-gap, design, leakage inductance, M4 steel, shunt reactor**

I. INTRODUCTION

SHUNT REACTORS are widely used in power grids for reactive compensation, harmonic filtration etc. They mostly have gapped iron core with distributed air-gaps along the limb. Equivalent circuit for a Gapped Iron-core Shunt-Reactor (GISR) is given in Fig. 1, where L_l is leakage, L_c is core and L_g is total air-gap inductance, whereas R_w ,R_c and R_g are the resistances representing winding, iron and gap losses [1].

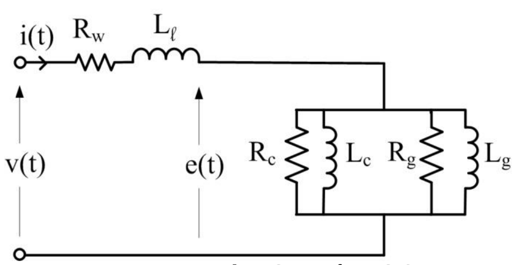

Fig.1. Equivalent Circuit for a GISR

A simple and practical analytical calculation for leakage inductance component of GISR does not exist in the literature; therefore this component is mostly neglected in the design phase and analysis. Influence of core gap in design of current limiting transformers is presented in [2] but leakage inductance component is not considered. Leakage inductance is neglected in another shunt reactor design study [3]. Although the leakage fields are considered in [4] determination of leakage inductance is not studied. Leakage inductance component is usually neglected in the studies on design of GISR including influence of dimensional parameters, design optimization, stress characteristics, etc. [5-8]. Finite Element Analysis (FEA) is widely used in GISR studies [9-12]. Determination of inductance components including leakage inductance by FEA is performed in [1] and [12], where calculation is based on energy method. A family of graphical curves called nomographs representing the variation of leakage inductance component in percentage against reactive power in terms of four different operating voltages and three different temperature rise values are presented in [12,13] for M330-35 AP Non-Grain-Oriented (NGO) steel (will be called M33 steel hereafter) by FEA. The proposed design criteria in this study is minimum Present Value Cost (min PVC). Presented results show that ratio of leakage inductance in the total amount may be significant. Therefore, neglecting the leakage inductance component in the design phase will result in a bulky and costly core.

In this work, leakage inductance components for M120-27S Grain-Oriented (GRO) steel (will be called M4 steel hereafter) by the method proposed in [12, 13] are calculated and presented as graphical curves. A design tool for single-phase GISR in Matlab/Guide is developed for analytical calculations. As a result, physical dimensions of the GISR under design are obtained for FEA. FEA are performed for various GISR with several operating voltages and temperature rise values to determine the leakage inductance component.

Since such information in the literature exist only for M33 steel as core material, the results presented in this work are beneficial for the design of GISR with M4 steel as an alternative core material. In addition, the developed design tool provides a practical and accurate design of such reactors.

II. METHODOLOGY

A. Design Tool for Analytical Calculations

Leakage inductance percentage values are calculated by FEA, therefore physical dimensions of the GISR under design are

ATİLLA DÖNÜK is with Department of Electrical & Electronics Engineering of Aydın Adnan Menderes University, Aydın, Turkey,(e-mail: adonuk@adu.edu.tr).

https://orcid.org/0000-0001-9468-8456

Manuscript received November 13, 2019; accepted April 23, 2020.
DOI: 10.17694/bajece.646625

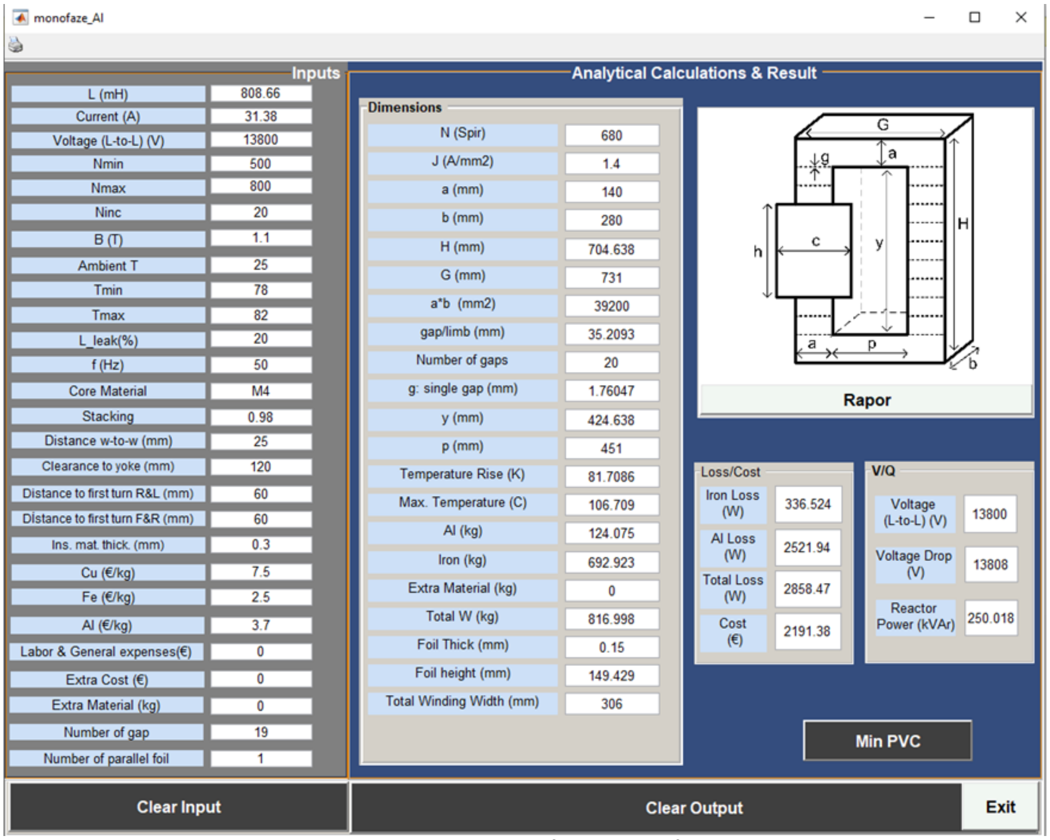

Fig.2. General overview of the design software

required for proper modelling in Maxwell 3D software. To obtain the physical dimensions, a design tool ware for analytical calculations is developed in Matlab/Guide environment as shown in Figure 2. The input data such as target inductance value, operating current and line-to-line voltage, minimum and maximum values of number of turns with incremental step, magnetic field density, ambient temperature, tolerances for temperature rise, leakage inductance percentage, operating frequency, type of core material, stacking factor, distances and clearances between coils and yoke, insulation material thickness, per-kg prices for core and winding materials, number of air-gaps and number of parallel foils for the GISR under design are to be entered by user. Extra data for labor and general expenses and extra cost of additional material can also be added.

Similar assumptions, for each set of operating voltages, such as

- Clearances
  - ➢ between yokes
  - ➢ between windings
  - ➢ between tube and windings
- insulation thickness
- tube thickness
- temperature rise values (60, 80 and 100 K with ±2 K tolerances)
- number of air-gaps in the core (40 in both the design and FEA analysis)
- aluminum foil as winding material
- operating magnetic flux density as 1.1 Tesla
- prices of iron and aluminum are taken to be 2.5 and 3.7 € per kg, respectively
- optimization criteria (min PVC)

defined in [12] are considered in the design phase. This will provide comparison of the leakage inductance percentage results in two different core materials, M33 and M4. Magnetization and loss curves for M4 steel provided by the manufacturer are given in Figure 3. B-H curve required for FEA analysis software is defined from the magnetization curve in Figure 3. Core loss calculation in the analytical design phase is performed as defined in Equation (1) which is obtained via curve fitting of the total loss characteristic given in Fig.3.

$$P_c = 0.41\, B^{1.7973} \text{ W/kg} \qquad (1)$$

After completing data entry, by pressing Min PVC button on the software screen given in Fig.2, the analytical calculation is started. The procedure is as follows:
Four different loops, from outer to inner, exist in the analytical calculation, such as:
• N, number of turns: minimum, maximum values and incremental rate are to be determined as input data by designer
• a, ratio of limb depth to limb width: from 1 to 2 with an incremental rate of 0.1
• t, foil thickness : from 0.05 to 1.0 with an incremental rate of 0.1
• J, current density: from 0.1 to 5 with an incremental rate of 0.1

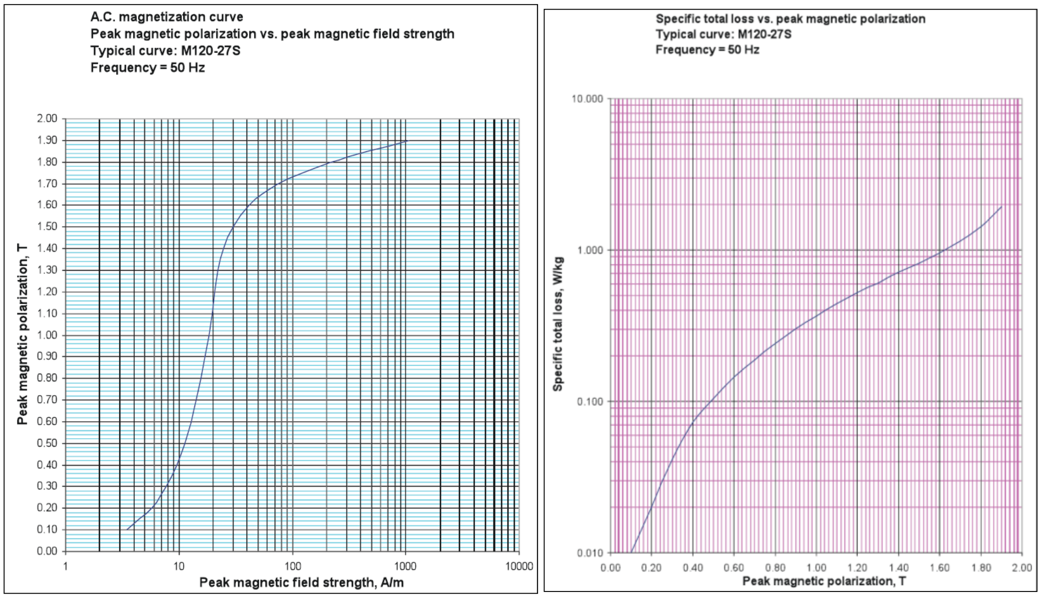

Fig.3. Magnetization and Loss Curves of M4 steel

The following design example can be considered for better understanding of the design process. A 250 kVAR 13800 V (808.66 mH, 31.38A) shunt reactor is to be designed. Input data and post-calculation results are as in Figure 2 and also summarized in Table I.

The core material for this design example is M4 steel and the winding material is Aluminum foil. Desired value of operating magnetic flux density is 1.1 Tesla, minimum and maximum temperature rise values are set at 78 and 82, respectively for 80 K temperature rise. Leakage inductance percentage is selected as 20 percent. Setting the initial number of turns (N) to 500 up to 800 with 20 incremental step, the software starts calculation with all data input given in Figure 2. After all iterations completed in almost a minute, the software will determine the optimum reactor satisfying the optimization criteria among thousands of reactors (N*a*t*J = 16*10*20*50=160000). At each iteration step firstly physical dimensions of the reactor, secondly core and winding losses, then Present Value Cost (PVC) and finally temperature rise are calculated. Since the design criteria is Min PVC, the reactor with minimum PVC among the reactors satisfying the desired temperature rise limit is determined as the optimum one and its calculated physical parameters are displayed on the screen

The results show that the optimum for defined assumptions; has 680 turns, 39200 mm2 cross-sectional area (limb width 140 mm and depth 280 mm, ratio of depth to width is 2). The software rounds the value of limb width to multiples of ten to satisfy the realistic steel dimensions used in practice. Prices of iron and aluminum are taken to be 2.5 and 3.7 € per kg, respectively. It is worth to note that the proposed design software provides all the input data and design criteria to be modified according to the special design under consideration.

The analytical results obtained from design software will be used as physical dimensions for modelling the reactor with Ansys/Maxwell software in determination of leakage inductance percentages of GISR.

B. Finite Element Analysis to Obtain Leakage Inductance Percentages

Firstly, physical dimensions and parameters of the reactor under design are obtained with the aid of the design software (Fig.2) and then the reactor is modelled in Maxwell 3D software to calculate inductance components by energy method as defined in [1, 12]. Table I represents target reactor specifications (design data), analytical calculation results obtained via the design software and FEA results for a set of iterations which are performed to obtain the leakage inductance percentage values for various power rating at 13.8 kV operating voltage, and at 80 K temperature rise. Each column in Table I represents an individual iteration, thus an individual reactor design phase. Since the estimated leakage inductance value changes at each new iteration, the physical parameters differs from each other.

Since the leakage inductance percentage is not known, design starts with an initial estimate. For the design of 250 kVAR 13.8 kV (808.66 mH, 31.38 A) GISR, initial estimate of leakage inductance at first is set to 5% as given in the first column of Table I. Then the analytical calculations with this value for the reactor are performed via the design software (Fig.2). After the physical parameters of the target reactor are obtained from analytical calculations, the reactor is then modelled in Ansys/Maxwell 3D software. Once FEA is performed, inductance parameters are obtained by the energy method. FEA results, shown at the end of the first column of Table I, show that the leakage inductance percentage and the inductance decline for this design iteration are 19% and 17%, respectively. However, two criteria

- leakage inductance percentage value close to the initial estimate
- inductance decline value smaller or equal to 5%

should be simultaneously satisfied for the iteration to be accurately completed;

TABLE I
DESIGN DATA / ANALYTICAL CALCULATION AND FEA RESULTS FOR A SAMPLE SET OF ITERATIONS WITH 13.8 KV OPERATING VOLTAGE AND 80 K TEMPERATURE RISE

Design Data								
Temparature Rise	80	80	80	80	80	80	80	80
# gap	40	40	40	40	40	40	40	40
kVAR	250	250	250	500	500	500	750	750
Voltage (l-l) kV	13,8	13,8	13,8	13,8	13,8	13,8	13,8	13,8
Current Amps	31,4	31,4	31,4	62,8	62,8	62,8	94,1	94,1
L (mH)	808	808	808	404	404	404	270	270
Analytical Calculation Results								
Lleak	0,05	0,1	0,2	0,05	0,1	0,15	0,1	0,15
Bm (T)	1,1	1,1	1,1	1,1	1,1	1,1	1,1	1,1
A (mm^2) ($x10^3$)	45	39,2	39,2	57,8	57,8	57,8	72,2	68,6
A_eff (mm^2) ($x10^3$)	44,1	38,4	38,4	56,6	56,6	56,6	70,8	67,2
foil thickness (mm)	0,15	0,15	0,15	0,25	0,25	0,25	0,3	0,3
J (A/mm^2)	1,4	1,3	1,4	1,1	1,2	1,2	1,1	1,1
height (mm)	729	717	705	865	837	842	971	968
N (turns)	730	730	680	550	490	500	420	410
l_gap (mm)	39,2	36,1	35,2	57,2	47,9	52,8	66,0	63,2
winding width (mm)	329	329	306	303	270	275	252	246
window (mm)	474	474	451	448	415	420	397	391
a (mm)	150	140	140	170	170	170	190	190
b (mm)	300	280	280	340	340	340	380	361
Temp Rise (K)	82	81,5	81,7	82	81,7	82	81,7	81,7
wind-wind clear. (mm)	25	25	25	25	25	25	25	25
yoke clearance (mm)	120	120	120	120	120	120	120	120
tube (mm)	60	60	60	60	60	60	60	60
PVC (euro)	2518	2421	2191	3912	3745	3570	4914	4720
Simulation Results								
L_total (mH)	944,8	892,7	789,8	470,4	434,3	418	291	273,5
L_gap (mH)	765,7	725	644,6	383,3	362,9	342,9	242,1	228,7
L_iron (mH)	1,69	1,82	1,55	0,62	0,68	0,57	0,34	0,33
L_leakage (mH)	177,5	165,9	143,6	86,5	70,7	74,6	48,5	44,3
Leakage %	18,8	18,6	18,2	18,4	16,3	17,8	16,7	16,2
Inductance decline %	16,85	10,39	2,34	16,33	7,40	3,38	7,96	1,42

Since the solution is not satisfying, a second iteration with the information given in the second column of Table I is performed for the same GISR. Now, initial leakage percentage is estimated to be 10% and defined as input data into the design software for analytical calculations. With the new set of physical parameters obtained for this case, the same procedure is repeated. Post-simulation results in the second column of Table I show that the inductance decline and the leakage inductance percentage criteria after the second iteration have not been met yet. Finally, a new design iteration and FEA are performed with 20% leakage inductance percentage estimation. Criteria to finalize the design for this individual reactor are finally satisfied in this third iteration, as being 18.18% leakage inductance and 2.34% inductance decline as shown in the third column of Table I.

Table I shows only a few iteration to explain the procedure in determining the leakage inductance percentage values. The process is repeated for each set of operating voltages, temperature rise values and power rating. As a result, hundreds of design and simulation iteration are performed to obtain leakage inductance percentages as graphical curves given in Figure 5.

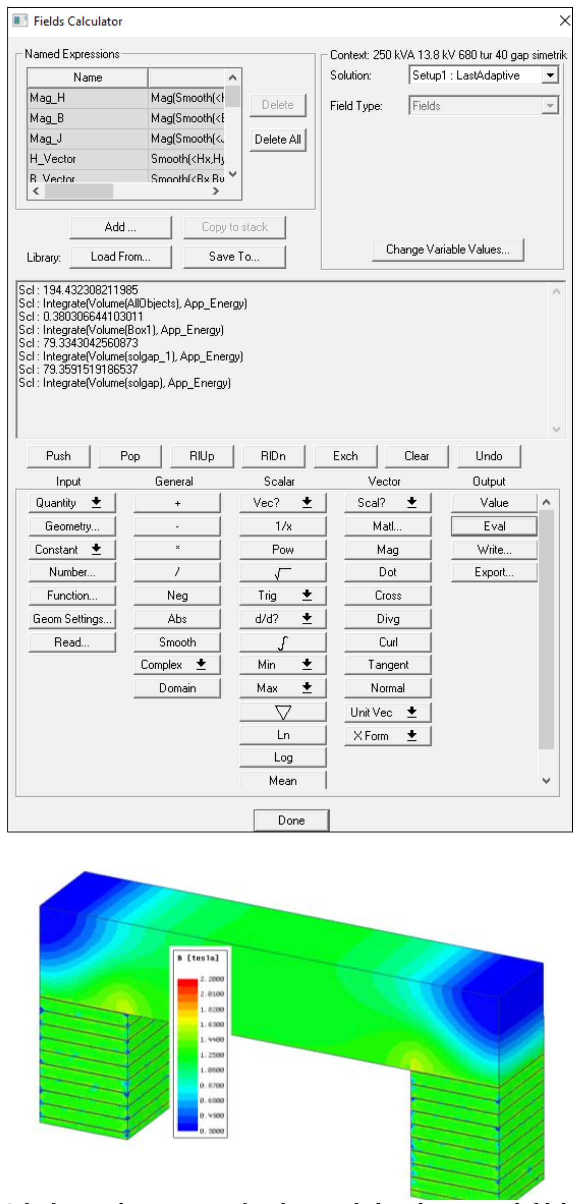

Fig.4. Calculation of energy in each volume and plot of magnetic field density for 250 kVAR 13.8 kV GISR with 20% leakage inductance and 80 K temperature rise

Calculation of inductance percentages in FEA are performed by energy method [1, 12]. The energy (co-energy may also be used for linear operation which is the case in general) in each volume; occupied by iron, air-gaps, and the total volume surrounding the core is calculated by integrating the energy density after post-simulation via the fields calculator of the software as shown in Fig.4. After having the resultant energy value, the inductance of the related volume is obtained by (2). By this way, all the inductance components of the GISR are obtained. Calculation of energy in each volume and plot of magnetic field density for 250 kVAR 13.8 kV GISR with 20% leakage inductance and 80 K temperature rise are given in Figure 4.

$$W = \frac{1}{2} L I^2 \tag{2}$$

C. Leakage Inductance Percentages as Graphical Curves

Variations in leakage inductance percentage against reactive power in terms of operating voltage and temperature rise for M4 steel are graphically represented in Figure 5. In addition, the graphs for M33 steel are given in Figure 5 [12] for comparison.

Leakage inductance percentage of M4 steel at 0.4 kV operating voltage is almost same for all temperature rise values up to 0.1 MVAR and beyond this power range it slightly increases. However, for M33 steel, leakage inductance percentages are different for all temperature values and increases dramatically. For M4 steel, leakage inductance percentage is lower at 80 K and 100 K, however, it is higher at 60 K temperature rise.

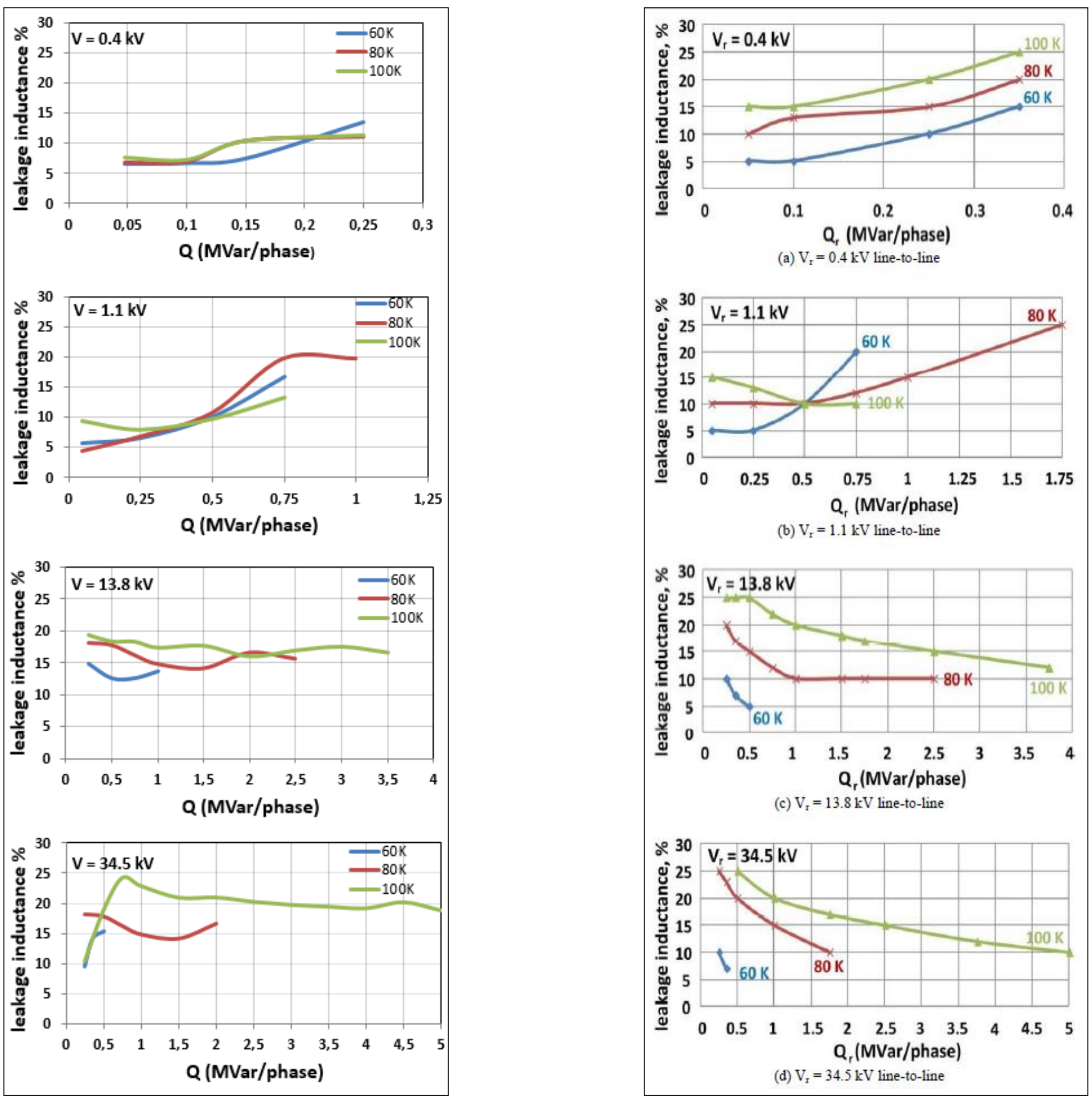

a. M4 steel

b. M33 steel [12]

Fig.5. Leakage inductance % of M4 steel and M33 steel

At 1.1 kV, leakage inductance percentage increases as reactive power increases for all temperature rise values, beyond 250 kVAR/phase for M4 steel and 500 kVAR/phase for M33 steel.

At 500 kVAR/phase, leakage inductance percentage seems to be 10 both for M4 and M33 steel for all temperature rise values.
At 13.8 kV, leakage inductance percentage decreases slightly for all temperature rise values for both materials, whereas the decrease is more dramatical for M33 steel.
The curves at 34.5 kV show considerable difference in behavior of two materials. Although the leakage inductance percentage values of M4 steel are lower at 0.4, 1.1 and 13.8 kV operating voltage, they are getting higher at 34.5 kV level as reactive power increases.
Graphical results show that both steel has its specific leakage inductance percentage values. Any change in core material during the design phase therefore requires new set of graphical curves for reliable results.

III. Conclusion

Neglecting leakage inductance in the design phase of GISR results in an expensive and bulky device as shown by presented simulation results. Graphical curves representing leakage inductance percentages for M4 steel in addition to the existing curves for M33 steel, will offer variety to the literature in design of GISR. Results presented in this work will provide manufacturers and designers to implement a fast, accurate and economical design by taking the effect of leakage inductance into consideration. The proposed design software for analytical calculations is a valuable design tool and provides design of GISR in a wide range.

Acknowledgment

This work has been funded by the Scientific and Technological Research Council of Turkey (TUBITAK) Code 1002 Grant in the scope of project 118E687.

References

[1] Atilla Donuk, Mihai Rotaru, Jan K. Sykulski, "Defining and computing equivalent inductances of gapped iron core reactors." Przegląd Elektrotechniczny (Electrical Review), vol.88.7b, 2012, pp.52-55.
[2] Lee R., Stephens D., "Influence of core gap in design of current limiting transformers." IEEE Transactions on Magnetics, vol. 9.3, 1973, pp. 408-410.
[3] J.P. Vora, H.C. Barnes, B.L. Johnson, "New shunt reactor principle proved-design data and factory test results for units built on insulated core principle." IEEE Transactions on Power Apparatus and Systems, Vol. PAS-92.3, 1973, pp. 900-906.
[4] B. Tomczuk, K. Babczyk, "Calculation of self and mutual inductances and 3-D magnetic fields of chokes with air gaps in core." Electrical Engineering, vol. 83, 2001, pp. 41-46.
[5] A. Bossi, G. Tontini, F. Coppadoro, "Influence of dimensional parameters on the design of gapped-core shunt reactors." IEEE Transactions on Power Apparatus and Systems, vol. 98.4, 1979, pp. 1144-1144.
[6] A. Lotfi, M. Faridi, "Design optimization of gapped-core shunt reactors." IEEE Transactions on Magnetics, Vol. 48.4, 2012, pp. 1673-1676.
[7] Y. Zhao, F. Chen, X. Ma, Z. Zhou, "Optimum design of dry-type air-gapped iron-core reactor based on dynamic programming and circular traversing algorithm." International Conference on Electromagnetic Field Problems and Applications, Dalian, Liaoning, China, 2012.
[8] B. Tong, Y. Qingxin, Y. Rongge, Z. Lihua, Z. Changgeng, "Research on stress characteristics of shunt reactor considering magnetization and magnetostrictive anisotropy." IEEE Transactions on Magnetics, vol.54.3, 2018.
[9] H.J.Kim, G.H. Lee, C.H. Jang, J.P. Lee, "Cost-effective design of an inverter output reactor in ASD applications." IEEE Transactions on Industrial Electronics, vol. 48.6, 2001, pp. 1128-1135.
[10] W.A. Roshen, "Fringing field formulas and winding loss due to an air gap." IEEE Transactions on Magnetics, vol. 43.8, 2007, pp. 3387-3394.
[11] H.D. Gersem, K. Hameyer, "A finite element model for foil winding simulation." IEEE Transactions on Magnetics, vol. 37.5, 2001, pp. 3427-3432.
[12] Atilla Dönük, *Modeling and Design of Iron-Core Shunt Reactors with Discretely Distributed Air-Gaps*, Middle East Technical University, 2012.
[13] A. Donuk, H.F. Bilgin, M. Ermis, "A practical approach to the design of power shunt-reactors with discretely distributed air-gaps." International Review of Modelling and Simulations, vol.6.2, 2013, pp. 567-576.

Biographies

ATİLLA DÖNÜK was born in Malatya, Turkey, in 1977. He received BS degree in Electrical and Electronics Engineering from Inönü University in 2000, and PhD degree in Electrical and Electronics Engineering from Middle East Technical University in 2012 where he has been a Research Assistant between September 2002 and February 2013. He worked as a guest researcher in the Research Group of Power Systems in Electrical and Computer Science at University of Southampton (UK) between November 2010 and October 2011. He has worked in Department of Electrical-Electronics Engineering at Atatürk University between February 2013 and July 2013. Since July 2013, he has been working as assistant professor in Department of Electrical and Electronics Engineering at Adnan Menderes University. His research interests include electrical machine design, power electronics and renewable energy applications.